

# Towards energy efficiency and maximum computational intensity for stencil algorithms using wavefront diamond temporal blocking

Tareq Malas

*Extreme Computing Research Center (ECRC)  
King Abdullah University of Science and Technology  
Thuwal, Saudi Arabia  
tareq.malas@kaust.edu.sa*

Georg Hager

*Erlangen Regional Computing Center (RRZE)  
Friedrich-Alexander University of Erlangen-Nuremberg  
Erlangen, Germany  
georg.hager@fau.de*

Hatem Ltaief

*Extreme Computing Research Center (ECRC)  
King Abdullah University of Science and Technology  
Thuwal, Saudi Arabia  
hatem.ltaief@kaust.edu.sa*

David Keyes

*Extreme Computing Research Center (ECRC)  
King Abdullah University of Science and Technology  
Thuwal, Saudi Arabia  
david.keyes@kaust.edu.sa*

**Abstract**—We study the impact of tunable parameters on computational intensity (i.e., inverse code balance) and energy consumption of multicore-optimized wavefront diamond temporal blocking (MWD) applied to different stencil-based update schemes. MWD combines the concepts of diamond tiling and multicore-aware wavefront blocking in order to achieve lower cache size requirements than standard single-core wavefront temporal blocking. We analyze the impact of the cache block size on the theoretical and observed code balance, introduce loop tiling in the leading dimension to widen the range of applicable diamond sizes, and show performance results on a contemporary Intel CPU. The impact of code balance on power dissipation on the CPU and in the DRAM is investigated and shows that DRAM power is a decisive factor for energy consumption, which is strongly influenced by the code balance. Furthermore we show that highest performance does not necessarily lead to lowest energy even if the clock speed is fixed.

**Keywords**- stencil algorithms; temporal blocking; performance modeling; energy efficiency

## I. INTRODUCTION

Regular stencil computations are major contributors to the runtime of many scientific applications. They arise as kernels in structured grid finite-difference and finite-volume discretizations of partial differential equation conservation laws and constitute the principal innermost kernel in many temporally explicit schemes for such problems. They also arise as a co-principal innermost kernel of Krylov solvers for temporally implicit schemes on regular grids. In iterative stencil computations, each point in a multi-dimensional spatial grid is updated using weighted contributions from its neighbor points, defined by the stencil operator. The stencil operator specifies the relative coordinates of the contributing points and their weights. The weights can be constant or variable in space and/or time with some or no symmetry

to be exploited around the updated point. The grid update operation over the complete spatial domain (one “sweep”) is repeated over many time steps (or iterations).

A high bytes-per-flop requirement is a prominent property of many stencil computations. It can be quantified by means of the *code balance* metric, i.e., the number of bytes transferred over a relevant bottleneck (usually the memory interface) divided by the “work” that can be done using this data. Since the number of flops may vary in stencil computations due to different formulations of the loop kernel or even compiler optimizations, the “lattice site update” (LUP) is a better metric for quantifying work. Hence, the code balance is measured in bytes/LUP. Its inverse is commonly called “computational intensity.” These metrics can be used to predict the performance of a loop code in a bandwidth-bound scenario [1]: the maximum memory-bound performance is the ratio of maximum memory bandwidth and the code balance.

At a large code balance, the increasing gap between computation and memory performance in contemporary and future high performance computing systems results in low hardware (i.e., CPU) utilization. The development of algorithms that can run stencil computations efficiently by reducing the code balance is thus essential for making better use of the hardware. At the same time, energy consumption and power dissipation are getting more attention in scientific computing due to the increasing energy and infrastructure cost for large systems. Performance and energy considerations are strongly intertwined, and any advancement in understanding the former will also help in controlling the latter.

Listing 1: 1<sup>st</sup>-order-in-time 7-point constant-coefficient isotropic stencil in three dimensions, with symmetry.

```
#pragma omp parallel for
for(int k=1; k < N-1; k++) {
  for(int j=1; j < N-1; j++) {
    for(int i=1; i < N-1; i++) {
      U[k][j][i] = c0 * V[k][j][i]
        + c1 * ( V[ k ][ j ][i+1]+ V[ k ][ j ][i-1])
        + c1 * ( V[ k ][j+1][ i ]+ V[ k ][j-1][ i ])
        + c1 * ( V[k+1][ j ][ i ]+ V[k-1][ j ][ i ]);
    }
  }
}
```

Listing 2: 1<sup>st</sup>-order-in-time 7-point variable-coefficient stencil in three dimensions, with no coefficient symmetry.

```
#pragma omp parallel for
for(int k=1; k < N-1; k++) {
  for(int j=1; j < N-1; j++) {
    for(int i=1; i < N-1; i++) {
      U[k][j][i] = C0[k][j][i] * V[k][j][i]
        + C1[k][j][i] * V[ k ][ j ][i+1]
        + C2[k][j][i] * V[ k ][ j ][i-1]
        + C3[k][j][i] * V[ k ][j+1][ i ]
        + C4[k][j][i] * V[ k ][j-1][ i ]
        + C5[k][j][i] * V[k+1][ j ][ i ]
        + C6[k][j][i] * V[k-1][ j ][ i ];
    }
  }
}
```

### A. Tested stencil cases

We perform our model validation and energy analysis using three “corner case” stencils: the 7-point constant-coefficient stencil in Listing 1, which operates at two domain-sized arrays to perform the Jacobi-like update, the 7-point variable-coefficient stencil in Lst. 2, which loads and caches an additional 7 domain-sized coefficient arrays, and the 25-point variable-coefficient stencil in Lst. 3, which operates on 13 coefficient arrays. These stencils are corner cases in the sense of including short- and long-range stencils and constant- and variable-coefficient stencils. Compared to the short-range stencils, the stencil operator of the long-range stencils includes more grid points (larger “stencil radius”) and has data dependency over more distant points in space from the updated lattice site, which adds more challenges for temporal blocking techniques. The variable-coefficient stencils have a several times higher data requirement per grid point compared to the constant-coefficient stencils, as they have to load the coefficient arrays, causing more cache pressure when using blocking techniques.

### B. Contribution

This work makes the following relevant contributions:

- We introduce a traffic model for stencil codes optimized with multicore wavefront diamond temporal blocking. The model predicts the data volume over the memory

Listing 3: 1<sup>st</sup>-order-in-time 25-point variable-coefficient anisotropic stencil in three dimensions, with symmetry across each axis.

```
#pragma omp parallel for
for(int k=4; k < N-4; k++) {
  for(int j=4; j < N-4; j++) {
    for(int i=4; i < N-4; i++) {
      U[k][j][i] = C00[k][j][i] * V[k][j][i]
        +C01[k][j][i]*(V[ k ][ j ][i+1]+V[ k ][ j ][i-1])
        +C02[k][j][i]*(V[ k ][j+1][ i ]+ V[ k ][j-1][ i ])
        +C03[k][j][i]*(V[k+1][ j ][ i ]+ V[k-1][ j ][ i ])
        +C04[k][j][i]*(V[ k ][ j ][i+2]+ V[ k ][ j ][i-2])
        +C05[k][j][i]*(V[ k ][j+2][ i ]+ V[ k ][j-2][ i ])
        +C06[k][j][i]*(V[k+2][ j ][ i ]+ V[k-2][ j ][ i ])
        +C07[k][j][i]*(V[ k ][ j ][i+3]+ V[ k ][ j ][i-3])
        +C08[k][j][i]*(V[ k ][j+3][ i ]+ V[ k ][j-3][ i ])
        +C09[k][j][i]*(V[k+3][ j ][ i ]+ V[k-3][ j ][ i ])
        +C10[k][j][i]*(V[ k ][ j ][i+4]+ V[ k ][ j ][i-4])
        +C11[k][j][i]*(V[ k ][j+4][ i ]+ V[ k ][j-4][ i ])
        +C12[k][j][i]*(V[k+4][ j ][ i ]+ V[k-4][ j ][ i ]);
    }
  }
}
```

bus, and thus the computational intensity, on a multi-core processor.

- We show by direct measurements that the model is correct as long as the required cache block size is within half the available cache size. This means that the MWD technique is able to attain the predicted memory traffic reductions.
- We show by direct measurements on the Intel Ivy Bridge processor that energy to solution for the considered optimized stencil codes correlates strongly with execution time, but that this apparently simple dependency is the result of two counteracting effects: a weak dependence of CPU power on the code performance and a strong dependence of DRAM power on the memory traffic.

## II. BACKGROUND

### A. Multicore wavefront diamond temporal blocking

We perform energy and code balance analysis in this paper using our proposed approach in [2]. It combines the concepts of diamond tiling and multi-core aware wavefront temporal blocking to construct Multi-core Wavefront Diamond blocking (MWD) for optimizing practically relevant stencil algorithms.

Our approach builds on a technique introduced by Strzodka *et al.* [3]. They combine diamond tiling with single-threaded wavefront temporal blocking. Our approach replaces the single-core wavefront with the multi-core wavefront proposed by Wellein *et al.* [4], which provides additional dimension of concurrency and offers large reduction in the cache block size and memory bandwidth requirements, as we shown in the results of our previous work [2].

In Figure 1 we illustrate the concept of diamond tiling for a one-dimensional 3-point stencil. Arrows represent the

data dependency across the diamond tiles. Diamond tiling provides convenient and unified data structure to maximize the in-cache data reuse [5], has low synchronization requirements, allows concurrent diamond tiles update, and can be utilized to perform domain decomposition in distributed memory setup.

The MWD space-time tile has the shape of an extruded diamond, as shown in Figure 2. The “frontlines” parameter determines the number of updated grid points in the wavefront direction per thread per time step in the wavefront update. The fading gray color represents recently updated grid points, with the darkest assigned to the most recent update. The wavefront traversal is performed along the  $z$  dimension (outer dimension) and the diamond tiling is performed across the  $y$  dimension (middle dimension). The  $x$  dimension (which is represented by single point in the figure) is left intact to have more contiguous memory accesses for efficient hardware data prefetching and reduced TLB misses.

Threads are assigned to the extruded diamonds in groups (“thread groups”), similar to [4]. Multiple thread groups can run concurrently, updating different diamond tiles and observing inter-diamond dependencies. The thread group size parameter provides controllable tradeoff between concurrency and sharing of the loaded data from memory among the threads of the multi-processor. Diamond tiles are dynamically scheduled to the available threads. A FIFO queue keeps track of the available diamond tiles for updating. Threads pop tiles from this queue to update them. When a thread completes a tile update, it pushes to the queue its dependent diamond tile, if that has no other dependencies. The queue update is performed in an OpenMP critical region to avoid race conditions. Since the queue updates are performed infrequently, the lock overhead is negligible.

Selecting the diamond tile size and the number of frontlines updates is achieved through auto-tuning to achieve the best performance. To shorten the auto-tuning process, the parameter search space is narrowed down to diamond tiles that fit within a predefined cache size range. Several constraints are considered in selecting the auto-tuning test points, for example, having sufficient concurrency and integer number of diamond tiles in each row of diamond tiles.

### B. Performance and energy consumption on multicore processors

Power dissipation, energy to solution, and more advanced energy-related metrics have become additional optimization targets in high performance computing besides pure time to solution and resource efficiency. Fortunately, low time to solution often leads to low energy to solution when looking at a fixed set of resources such as a multicore CPU or a compute node. Modern multi-core processors have advanced power gating mechanisms that make their power dissipation highly dynamic and code-dependent. For

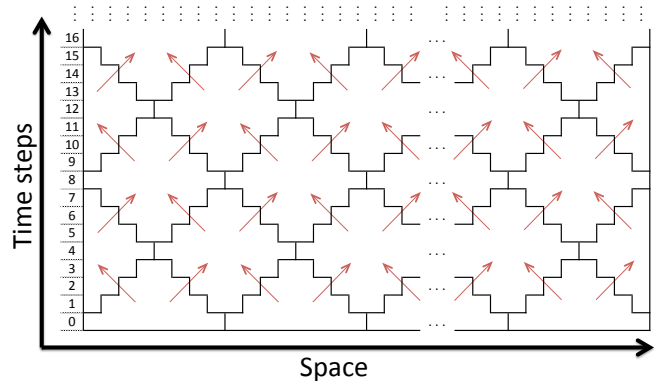


Figure 1: Diamond tiling on a one-dimensional space grid, with arrows representing inter-tile data dependencies. The number of diamond tiles per row represents the maximum attainable concurrency, as the tiles in the row can be executed independently of each other.

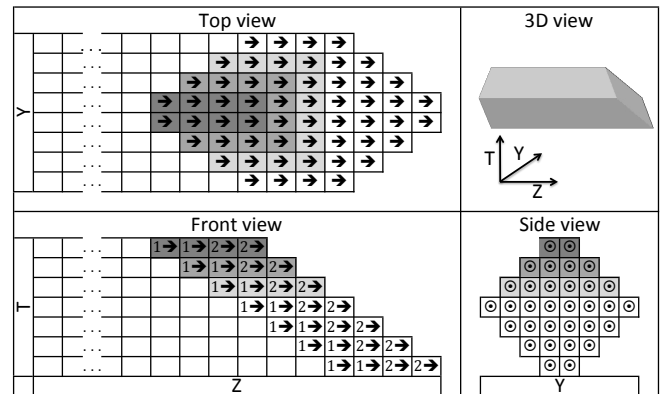


Figure 2: Diamond tiling with a multi-thread wavefront (shown here with two threads) in a three-dimensional space grid, using two frontlines per thread.

instance, idle cores (or parts of them) can be put into deep sleep states. Nevertheless there are successful attempts to describe their power behavior using simple models, which are not perfectly accurate but provide useful insights [6], [7]. We briefly summarize here the consequences of the energy model derived in [7]. It assumes a non-zero “baseline” or “static power,” which is the extrapolated power dissipation with all cores idling, and a constant per-core, code-dependent dynamic power contribution from every core that is not idle:

$$W = W_{\text{stat}} + n \cdot W_{\text{dyn}} . \quad (1)$$

One crucial property that influences energy consumption is the scaling behavior of a code (or rather an execution phase, which is often a loop nest) across the cores of a multicore chip. If performance scales across the cores, energy to solution is minimal when using all cores. On the other

hand, if the code performance saturates, like with strongly memory-bound loop kernels or imbalanced workload, lowest energy is achieved when using as many cores as required to saturate, but not more. If the saturation is caused by a hardware bottleneck (typically memory bandwidth), reducing the clock speed at larger core count will further decrease the energy to solution.

Given the plethora of relevant stencil variants and possible optimization techniques, it is impossible to pinpoint a generic energy behavior for “stencils at large,” since those cover the complete spectrum from fully scalable to strongly saturating. Modern hardware structures beyond the CPU chip with dynamic power behavior such as large DRAMs complicate matters further. In this work we show, using baseline and optimized implementations of three stencil-based algorithms, that the usual law of “faster code uses less energy”, or “race-to-halt” as defined by Hennessy and Patterson [8], is often but not always true.

### III. ANALYSIS AND OPTIMIZATION OF THE MWD ALGORITHM

#### A. Loop tiling for the leading dimension

The experiments of our MWD implementation in [2] showed a degradation in the thread scaling performance of the 7-point variable-coefficient stencil at grid size  $N=680^3$ , where the performance at 10 threads was lower than at 8 and 9 threads. Using half the leading dimension ( $N_x$ ) in other experiments (i.e.,  $340 \times 680 \times 680$ ) led to good performance scaling up to 10 threads. This is a result of reducing the cache block size to half, since  $N_x$  contributes linearly in the cache block size, as will be shown in Section III-C. Blocking in the leading dimension was thus considered to resolve the cache capacity issue. Reducing the leading dimension size can allow for more in-cache data reuse by fitting larger diamond tiles in the cache. This is especially useful when the memory bandwidth remains a bottleneck even with MWD.

To avoid adding more complexity in scheduling tiles to thread groups, the same thread group updates all the tiles in the leading dimension of its assigned extruded diamond sequentially. The implementation is kept simple by using parallelepiped tiles in the leading dimension.

The performance-optimal tile size in the leading dimension is problem-dependent, as small blocks can result in increased TLB misses and excess data volume due to hardware prefetching. To handle this issue, we incorporated the tile size selection in our auto-tuning implementation, to tune it along with the diamond tile size and the number of frontlines.

This tiling implementation can be found in the current code release of our framework [9].

#### B. Cache block size model

We consider the MWD wavefront cache block size model from [2] to validate its correctness and study its impact

on the code balance at different diamond sizes. The model calculations require four parameters: the diamond width  $D_w$  in the  $y$  axis, the wavefront frontlines number  $N_F$ , the bytes number in the leading dimension  $N_{xb}$ , the stencil radius  $R$ , and the number of domain-sized streams in the stencil operator,  $N_D$ . Examples of stencil radius are  $R = 1$  and  $R = 4$  at the 7- and 25-point stencils, respectively. The 7-point constant-coefficient stencil has  $N_D = 2$  (Jacobi-like update). The 7-point variable-coefficient stencil uses seven additional domain-sized streams to hold the coefficients. For a stencil with  $R=1$ , the wavefront width  $W_w$  has the size:  $W_w = D_w + N_F - 2$  and the total required bytes in the wavefront cache block  $C_S$ , with some approximations, is:

$$C_S = N_{xb} \cdot \left[ N_D \cdot \left( \frac{D_w^2}{2} + D_w \cdot (N_F - 1) \right) + 2 \cdot (D_w + W_w) \right]. \quad (2)$$

Here,  $N_{xb}$  is the size of the leading dimension tile size, and  $D_w^2/2 + D_w \cdot (N_F - 1)$  is the diamond area in the  $y$ - $z$  plane as shown in the top view of Figure 2. The halo region of the wavefront (i.e., the read-only grid points around the cache block) is  $2 \cdot (D_w + W_w)$ .

For example, we have  $D_w = 8$  and  $N_F = 4$  in Figure 2, so  $W_w = 8 + 4 - 2 = 10$  and the total block size at 7-point constant-coefficient stencil is  $N_{xb} \cdot (2 \cdot (8^2/2 + 8 \cdot 3) + 2 \cdot (8 + 10)) = 148 \cdot N_{xb}$  bytes.

The steeper wavefront in higher-order stencils results in different wavefront lengths ( $W_w = D_w - 2 \cdot R + N_F$ ) and different  $C_S$  as follows:

$$C_S = N_{xb} \cdot \left[ N_D \cdot D_w \cdot \left( \frac{D_w}{2} - R + N_F \right) + 2R(D_w + W_w) \right]. \quad (3)$$

It is worth mentioning that each thread group requires a dedicated  $C_S$  in the blocked cache level. For example, using 1WD in a 12-core Intel Ivy Bridge socket requires fitting  $12 \cdot C_S$  bytes in the L3 cache.

#### C. Memory traffic model

In order to validate the effectiveness of the bandwidth pressure reduction on the memory interface, we set up a model to estimate the code balance for the temporally blocked case. If the wavefront fits completely in the L3 cache, each grid point is loaded once from main memory and is stored once after updating it during the extruded diamond update. In this case, the amount of data transfers during the extruded diamond update consists of  $(2D_w - 2)$  data writes plus  $(N_D \cdot D_w + 2)$  data reads, all multiplied by  $N_z$ . The number of total LUPs performed through the diamond volume is:  $N_z \cdot D_w^2/2$ . The code balance at double precision of a stencil with  $R = 1$  is thus:

$$B_C = \frac{16 \cdot [(2D_w - 2) + (N_D \cdot D_w + 2)] \text{ bytes}}{D_w^2 \text{ LUP}}. \quad (4)$$

When  $R > 1$  the amount of data transfers becomes  $N_z \cdot [(2D_w - 2R) + (N_D \cdot D_w + 2R)]$  and the extruded

diamond volume becomes  $N_z \cdot D_w^2 / (2 \cdot R)$ . In total, the equation becomes:

$$B_C = \frac{16R \cdot [(2D_w - 2R) + (N_D \cdot D_w + 2R)] \text{ bytes}}{D_w^2 \cdot \text{LUP}} \cdot \quad (5)$$

## IV. RESULTS

### A. Test system and tools

All benchmark tests were performed on a cluster of dual-socket Intel Ivy Bridge (Xeon E5-2660v2) nodes with a nominal clock speed of 2.2 GHz and ten cores per chip. This processor has a maximum thermal design power (TDP) of 95 W. The “Turbo Mode” feature was disabled. Each CPU has a 25 MiB L3 cache which is shared among all cores, and core-private L2 and L1 caches of 256 KiB and 32 KiB, respectively. All data paths between the cache levels are half-duplex, 256-bit wide buses, so the transfer of one 64-byte cache line between adjacent caches takes two CPU cycles. The core architecture supports all Intel Single Instruction Multiple Data (SIMD) instruction sets up to AVX (Advanced Vector Extensions). With AVX, one core is able to sustain one full-width (32 byte) load and one half-width (16 byte) store per cycle. In addition, one AVX multiply and one AVX add instruction can be executed per cycle. Since one AVX register can hold either four double precision (DP) or eight single precision (SP) operands, the peak performance of one core is eight flops per cycle in DP or sixteen flops per cycle in SP.

Each node is equipped with 64 GB of DDR3-1600 RAM per socket and has a maximum attainable memory bandwidth of  $b_S \approx 40$  GB/s per socket (as measured with the STREAM COPY [10] [11] benchmark). The nodes are connected by a full non-blocking, fat-tree QDR InfiniBand network.

For compiling and linking, the Intel C compiler in version 13.1.3 was used. Hardware performance counter measurements were done with `likwid-perfctr` from the LIKWID multicore tools collection [12]. Apart from standard metrics, `likwid-perfctr` can also measure power dissipation and energy consumption based on the RAPL (Running Average Power Level) mechanism. RAPL is an energy model implemented in hardware with high degree of accuracy [13]. Its technology allows to measure energy seamlessly by using hardware counter technology available on Intel Sandy/Ivy Bridge lines of multicore processors. On the system used for the tests, RAPL is able to report CPU energy separately from DRAM energy. Note that RAPL has been designed not just for monitoring instantaneous energy consumption but also for capping the total energy and power at the software level.

### B. Code balance

In this section we verify the correctness of our memory traffic and cache block size models. The three stencils

described in Section I-A are used at realistic grid sizes.

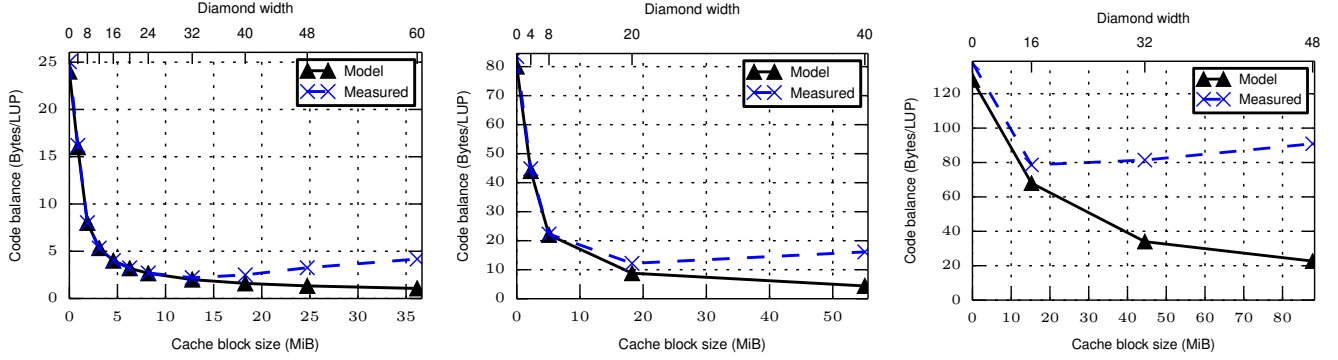
We use 10WD in our verification experiments, because it has the largest range of diamond tile sizes that fits in the L3 cache, where all the threads work in a single cache block. Smaller thread group sizes result in similar behavior, but run out of cache at smaller diamond sizes, as they require one cache block per thread group to co-exist in the cache memory. Hence, we omit those results since they do not add insight beyond 10WD. The number of frontlines is fixed to 10 across all experiments, which is the minimum allowed to run a 10-thread wavefront in our implementation.

Figure 3 shows cache block size vs. code balance at different diamond tile sizes, along with the corresponding diamond width (top  $x$  axis). The coordinates of each data point in the “Model” data sets is computed by evaluating the cache size model and code balance model at a given diamond width. The coordinates in the “Measured” data sets uses the actual measured code balance in place of the code balance model at the  $y$  axis. Multiples of valid diamond sizes are used in the measurements, where multiples of 4 and 16 are used for the 7-point and 25-point stencils, respectively. Several diamond sizes are omitted in the figures because they would require a non-integer number of tiles in the diamond-tiling dimension. For example,  $D_w = 12$  is omitted at Fig. 3b because 680 is not a multiple of 12. Data points at diamond width of zero correspond to a standard spatial blocking scheme.

Our models are very accurate in predicting the code balance of corner-case stencil operators. There is a strong agreement between the model and the empirical results when the cache block (i.e., wavefront) fits in the L3 cache (in the range of 12–18 MiB). This shows that our implementation of the MWD blocking scheme can actually achieve the theoretical memory traffic reductions. The measured code balance in Fig. 3 starts to deviate from the model at cache blocks larger than about half the Intel Ivy Bridge’s L3 cache size (i.e., 25 MiB). The deviation at this point can be predicted from our cache block size model, considering the rule-of-thumb that half the cache size is usually usable for blocking. This rule has emerged from experience for stencil codes that show an approximate balance of data volumes between the stencil array and other (streaming) data in the loop code. If the latter dominates the data volume, the factor of one half may be reduced.

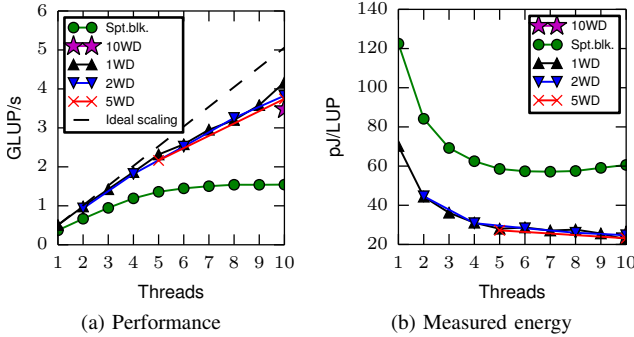
### C. Performance and energy consumption

Thread scaling data of the performance and the measured energy consumption for the three stencil operators under consideration are shown in Figures 4, 5, and 6. More detailed energy results, which separate CPU and DRAM power and energy, are listed in Tables I, III, and III for those core counts which lead to lowest energy consumption. Auto-tuning is used throughout the thread scaling experiments to find the performance-optimal set of parameters for each experiment.



(a) 7-point constant-coefficient stencil using grid size  $N = 960^3$  (b) 7-point variable-coefficient stencil using grid size  $N = 680^3$  (c) 25-point variable-coefficient stencil using grid size  $N = 480^3$

Figure 3: Cache block size vs. modeled code balance and measured code balance, evaluated at several diamond tile sizes using 10WD with three corner-case stencil operators.



(a) Performance (b) Measured energy

Figure 4: 7-point constant-coefficient stencil performance and energy. Grid size  $N = 960^3$ .

	Method	Spt. Blk.	1WD	2WD	5WD	10WD
	Threads	6	10	10	10	10
	MLUP/s	1448	4170	3825	3744	3481
Power [W]	CPU	42.10	58.00	63.45	57.75	56.76
	DRAM	40.93	35.82	31.12	28.95	27.44
	Total	83.03	93.81	94.56	86.70	84.20
Energy [pJ/LUP]	CPU	29.09	13.92	16.59	15.42	16.31
	DRAM	28.28	8.60	8.14	7.73	7.88
	Total	57.36	22.51	24.72	23.16	24.19

Table I: 7-point constant-coefficient stencil power dissipation and energy to solution

We observe that tiling in  $x$  does not achieve the desired performance improvements. The auto-tuner thus selects a full stride in  $x$  in most of the experiments. We attribute this failure to the hardware prefetching unit bringing in data beyond the block in  $x$ , which annihilates any advantage of the desired cache block size saving.

1) *7-point constant-coefficient stencil*: This stencil operator shows the usual strongly saturating performance with pure spatial blocking across the cores of the CPU chip (circles in Fig. 4a). We thus expect lowest energy to solution

at around six threads, which is confirmed by the measurements (circles in Fig. 4b). The corresponding column in Table I shows that the overall power is almost evenly distributed between CPU and DRAM. The variants with temporal blocking all have much better performance, and thus CPU utilization, but exert less pressure on the memory interface. Consequently, their CPU power is higher (between 58 W and 64 W) but their DRAM power is lower, with 10WD hitting the minimum at just over 27 W. In fact, 10WD has the lowest overall power of all WD codes.

Considering the power dissipation and performance numbers of all variants it is evident that spatial blocking must have the largest total energy consumption due to its low performance, and indeed the last row of Table I proves that all WD codes are more than a factor of two ahead in energy efficiency. 10WD, although it leaves the CPU and DRAM “cooler,” is still considerably slower than 1WD, which eventually causes a slightly worse energy efficiency. Thus, the general rule of “faster code is more energy efficient” seems to be confirmed for this case, but among the WD versions this result emerges from a complex interplay of performance and power dissipation between CPU and DRAM, and it may not hold for other stencil operators.

Note that due to their reasonably good scalability (see Fig. 4a), all WD codes show minimum energy to solution at the full socket (10 cores).

2) *7-point variable-coefficient stencil*: This stencil operator has the most unusual energy vs. performance characteristic. First of all, due to the saturating performance of 1WD the minimum energy operating point is at only eight cores for this code (triangles in Fig. 5). The 5WD variant, despite showing about 30% speedup from 5 to 10 cores, has lowest energy at five cores (crosses). In practice one would usually not favor lower energy over shorter time to solution, which is why we have included the 10-core power data in Table II. 5WD shows the energy advantage at 5 cores because it uses

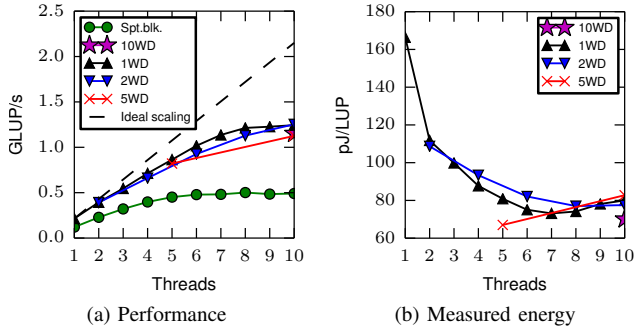


Figure 5: 7-point variable-coefficient stencil performance and energy. Grid size  $N = 680^3$ .

	Method	Spt. Blk.	1WD	2WD	5WD	10WD
	Threads	6	8	10	10	10
	MLUP/s	479	1214	1253	1126	1152
Power [W]	CPU	39.78	48.26	59.19	54.11	52.93
	DRAM	47.40	41.66	37.94	38.73	26.91
	Total	87.18	89.93	97.13	92.84	79.84
Energy [pJ/LUP]	CPU	83.14	39.79	47.25	48.23	46.49
	DRAM	99.07	34.35	30.28	34.52	23.63
	Total	182.21	74.14	77.53	82.76	70.12

Table II: 7-point variable-coefficient stencil power dissipation and energy to solution

a diamond width of  $D_w = 20$  compared to  $D_w = 8$  at 10 cores, resulting in more savings in memory bandwidth, which leads to lower DRAM power. This happens because more cache space is available per thread at 5 threads. The performance advantage at 10 threads is not large enough to compensate the larger DRAM and CPU power.

Comparing all variants with respect to energy consumption and performance, we see that although 2WD has best performance, 10WD shows lowest energy to solution, mainly due to its very low power dissipation in the DRAM. Since the DRAM accounts for a significant fraction of the overall power dissipation, the 7-point variable-coefficient stencil operator with its high memory pressure (i.e., large code balance) benefits not only in terms of performance but also in terms of energy, especially when using 10WD which has the lowest memory bandwidth utilization. However, its 6% energy advantage comes at the cost of an 8% performance loss compared to 2WD.

Although tiling in  $x$  is not generally improving the performance compared to [2], it prevents the performance degradation of the 7-point variable-coefficient stencil at 10 threads in Fig. 5a, where the best performance at 10 threads is achieved with a tile size of 340 (half the leading dimension size).

3) *25-point variable-coefficient stencil*: This is again a case where “fastest” also means “least energy.” The 10WD variant achieves best performance and lowest energy to solution for this stencil operator (see Fig. 6), because it is the

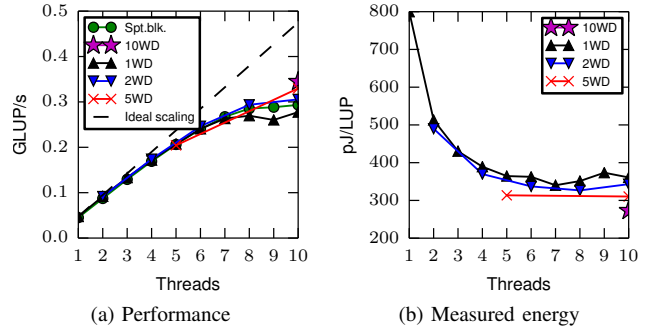


Figure 6: 25-point variable-coefficient stencil performance and energy. Grid size  $N = 480^3$ .

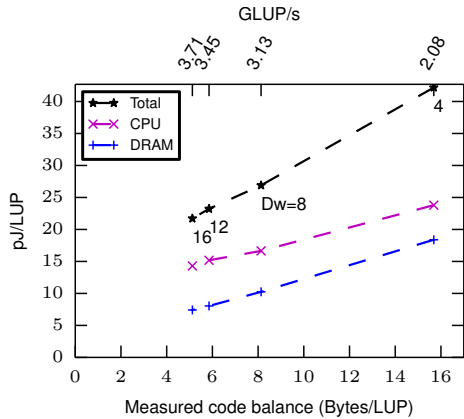
	Method	Spt. Blk.	1WD	2WD	5WD	10WD
	Threads	8	7	8	10	10
	MLUP/s	285	263	294	330	345
Power [W]	CPU	46.1	44.1	51.2	53.8	53.3
	DRAM	48.5	45.5	44.7	48.4	40.7
	Total	94.6	89.6	95.9	102.2	94.0
Energy [pJ/LUP]	CPU	161.8	167.3	174.4	163.3	154.8
	DRAM	170.2	172.8	152.2	147.1	118.2
	Total	331.9	340.2	326.5	310.4	273.0

Table III: 25-point variable-coefficient stencil power dissipation and energy to solution

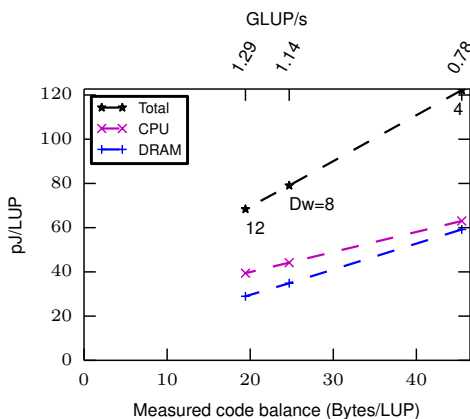
only code that shows significant power savings in DRAM (see Table III). 5WD, despite its substantial speedup from 5 to 10 cores, has the same energy to solution in both cases. The speedup is just barely sufficient to compensate for the additional power from the larger number of active cores.

4) *Code balance and energy consumption*: Although these findings would not justify favoring 10WD over all other options today and on the architecture under consideration, they show clearly that the expected future trends towards more bandwidth-starved systems and higher relative power dissipation in the memory subsystem should be met with algorithms that exhibit lowest possible code balance. This view is corroborated by another observation in our data: Across all stencil operators, the *overall* energy savings of temporal blocking vs. standard spatial blocking are roughly accompanied by equivalent runtime savings. But when the energy consumption of CPU and DRAM are inspected separately it is evident that this equivalence emerges from the mutual cancellation of two opposing effects: While the CPU energy is less strongly correlated with the code performance, the DRAM energy shows an over-proportional reduction for temporal blocking.

This can be seen more clearly in Fig. 7 where we have measured the energy to solution with respect to the code balance for 5WD (as a consequence of setting different diamond tile sizes) for both 7-point stencils (the diagram for the 25-point stencil would only contain a single data point per set). In both cases the DRAM energy depends much



(a) 7-point constant-coefficient stencil at grid size  $N = 960^3$ .



(b) 7-point variable-coefficient stencil at grid size  $N = 480^3$ .

Figure 7: Energy vs. code balance for the seven-point stencils at several diamond tile sizes, separately for DRAM and CPU and as a total sum. The corresponding performance of each experiment is shown on the top x-axis. The annotation at each point represents the used diamond width. 5WD is used in the experiments.

more strongly on the code balance than the CPU energy. This was expected from the observations described above, but the CPU energy dependence is far from weak. Overall there is an almost linear dependence of energy on code balance, making the latter a good indicator of the former.

## V. RELATED WORK

In 2009, Datta et al. [14] provide an exhaustive review of the state of research on stencil code optimizations. They cover the performance of several combinations of optimization techniques, processors, and stencil operators. Of all optimization options, temporal blocking is the most promising strategy since it allows for a dramatic reduction of code balance and, potentially, a decoupling from the memory bandwidth bottleneck. However, it is not straightforward to apply since it requires careful handling of inter-tile

dependencies. Many variants using different tile shapes have been developed in recent years. Reviews can be found in Orozco *et al.* [15] and Zhou [16]. The idea of diamond tiling has been investigated by several groups, e.g., Strzodka *et al.* [3], Bandishti *et al.* [17].

Wavefront-based blocking was introduced by Lamport [18] and combined with tiling strategies by other authors [3], [19], [20]. They all have in common that shared caches in modern multi-core processors are not leveraged for improved cache reuse. This was first introduced by Wellein *et al.* [4] with multicore wavefront temporal blocking. In recent work [2] we have combined this idea with previous work on diamond tiling to arrive at the MWD scheme which is used in this work.

Our approach to studying performance behavior of optimized stencil computations is based on a combination of auto-tuning (e.g., for selecting appropriate diamond sizes) and model-guided performance engineering, where we try to quantify the impact of bottlenecks on the code execution much along the lines of the well-known Roofline model [1]. The code balance (inverse computational intensity) is thus the ideal first-order metric for this.

The emergence of energy and energy-related metrics as new optimization targets in HPC has sparked intense research on power issues in recent years. For instance, the realization that low energy and low time to solution may be opposing goals has led to activities in multi-objective auto-tuning [21], [22]. However, there is very little work that tries to connect power dissipation with code execution using simple synthetic models to gain insight without statistical or machine learning components. Hager et al. [7] have constructed a simple power model that can explain the main features of power scaling and energy to solution on standard multicore processors. Choi et al. [6] follow a slightly different approach by modeling the energy consumption of elementary operations such as floating-point operations and cache line transfers. In this work we try to pick up some of those ideas to establish a connection between energy consumption on the CPU and in the DRAM with the performance and, more importantly, with the code balance of a stencil algorithm.

## VI. SUMMARY AND OUTLOOK

In this work we have established a memory traffic model for stencil update schemes that are optimized by Multi-core Wavefront Diamond (MWD) temporal blocking. Our traffic model can predict the optimal code balance as a function of the stencil radius, the diamond width, and the number of domain-sized streams. We have validated the model predictions on a 10-core Intel Ivy Bridge by direct traffic measurements for three stencil operators with different properties: a 7-point constant-coefficient stencil, a 7-point stencil with variable coefficients, and a long-range 25-point stencil with variable axis-symmetric coefficients. The model

is very accurate if the required cache block size (which is also predicted) fits into about half the shared outer level cache size. This enables a useful memory traffic calculation, and constitutes an important step towards improved model-guided automated tuning.

By direct energy measurements for CPU and DRAM using the RAPL facilities we could show that the DRAM power dissipation is a crucial factor for energy to solution on the system under consideration, and that it correlates strongly with the memory traffic. As a consequence, the general observation that there is an almost linear dependence between time and energy to solution may not always be true, even if the executed low-level code is identical. Indeed we have identified one case (7-point stencil operator with variable coefficients) where the most time-efficient MWD variant is not the most energy-efficient. Although these were not major deviations, the observed dependence on the DRAM power points to expected future trend towards a shift of power dissipation hot spots from execution resources to data resources. Algorithms like MWD with strongly reduced memory pressure stay abreast of these changes.

We present some final performance measurements in a different hardware setting to substantiate this point: Figure 8 shows the thread scaling performance of the 7-point variable-coefficient stencil on a single socket of a 12-core Ivy Bridge CPU in the “Edison” system at NERSC. The socket has a measured STREAM TRIAD bandwidth of  $b_S \approx 45$  GB/s and runs at a base clock speed of 2.4 GHz. Compared to the 10-core Intel Ivy Bridge we used in our earlier experiments, this system has a 12.5% higher memory bandwidth, 25% more cores, and a 10% higher clock speed. As a result, it is more bandwidth-starved, i.e., the ratio of memory bandwidth to peak performance is lower. As a result, MWD (and especially 12WD) shows a significant improvement in full-chip performance, much more than spatial blocking (which can only benefit from the 12.5% bandwidth boost).

The recent availability of the new Intel Haswell-EP processor will add a new twist to our study since the number of cores, peak performance, cache sizes, and (to a lesser extent) the memory bandwidth will all be increased considerably. We expect MWD to have even stronger advantages in terms of performance and energy on this new architecture.

#### ACKNOWLEDGMENT

The Extreme Computing Research Center at KAUST supported T. Malas. Part of this work was supported by the German DFG priority programme 1648 (SPPEXA) within the project Terra-Neo, and by the Bavarian Competence Network for Scientific High Performance Computing in Bavaria (KONWIHR) under the project OMI4papps. We are indebted to Jan Treibig and Thomas Röhl (RRZE) who provided support with the LIKWID tool suite. This research used resources of the National Energy Research Scientific

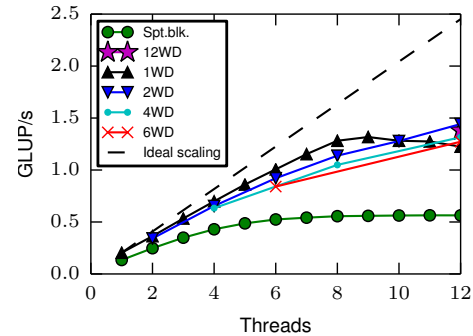


Figure 8: 7-point variable-coefficient stencil thread scaling performance at a 12-core Intel Ivy bridge processor at Edison supercomputer using grid size  $N = 680^3$ .

Computing Center, a DOE Office of Science User Facility supported by the Office of Science of the U.S. Department of Energy under Contract No. DE-AC02-05CH11231.

#### REFERENCES

- [1] S. Williams, A. Waterman, and D. Patterson, “Roofline: An insightful visual performance model for multicore architectures,” *Communications of the ACM*, vol. 52, no. 4, pp. 65–76, Apr. 2009. [Online]. Available: <http://doi.acm.org/10.1145/1498765.1498785>
- [2] T. Malas, G. Hager, H. Ltaief, H. Stengel, G. Wellein, and D. Keyes, “Multicore-optimized wavefront diamond blocking for optimizing stencil updates,” *ArXiv e-prints*, Oct. 2014.
- [3] R. Strzodka, M. Shaheen, D. Pajak, and H.-P. Seidel, “Cache accurate time skewing in iterative stencil computations,” in *Proceedings of the International Conference on Parallel Processing*. IEEE Computer Society, Sep. 2011, pp. 571–581.
- [4] G. Wellein, G. Hager, T. Zeiser, M. Wittmann, and H. Fehske, “Efficient temporal blocking for stencil computations by multicore-aware wavefront parallelization,” in *Computer Software and Applications Conference. 33rd Annual IEEE International*, vol. 1, July 2009, pp. 579–586.
- [5] D. Orozco and G. Gao, “Mapping the FDTD application to many-core chip architectures,” in *Proceedings of the International Conference on Parallel Processing*, Sept 2009, pp. 309–316.
- [6] J. W. Choi, D. Bedard, R. Fowler, and R. Vuduc, “A roofline model of energy,” in *International Parallel and Distributed Processing Symposium*. Washington, DC, USA: IEEE Computer Society, 2013, pp. 661–672. [Online]. Available: <http://dx.doi.org/10.1109/IPDPS.2013.77>
- [7] G. Hager, J. Treibig, J. Habich, and G. Wellein, “Exploring performance and power properties of modern multicore chips via simple machine models,” *Concurrency and Computation: Practice and Experience*, 2014. [Online]. Available: <http://dx.doi.org/10.1002/cpe.3180>

- [8] J. Hennessy, D. Patterson, and K. Asanović, *Computer Architecture: A Quantitative Approach*, ser. Morgan Kaufmann. Morgan Kaufmann/Elsevier, 2012, pp. 26. [Online]. Available: <http://books.google.com.sa/books?id=v3-1hVwHnHwC>
- [9] “Girih stencil optimization framework,” [https://github.com/tareqmalas/girih/releases/tag/IPDPS2014\\_submission](https://github.com/tareqmalas/girih/releases/tag/IPDPS2014_submission).
- [10] J. D. McCalpin, “STREAM: Sustainable memory bandwidth in high performance computers,” University of Virginia, Charlottesville, VA, Tech. Rep., 1991-2007, a continually updated technical report. [Online]. Available: <http://www.cs.virginia.edu/stream/>
- [11] —, “Memory bandwidth and machine balance in current high performance computers,” *IEEE Computer Society Technical Committee on Computer Architecture Newsletter*, pp. 19–25, Dec. 1995.
- [12] “LIKWID performance tools.” [Online]. Available: <http://code.google.com/p/likwid>
- [13] E. Rotem, A. Naveh, A. Ananthakrishnan, D. Rajwan, and E. Weissmann, “Power-management architecture of the Intel microarchitecture code-named Sandy Bridge,” *IEEE Micro*, vol. 32, pp. 20–27, 2012.
- [14] K. Datta, S. Kamil, S. Williams, L. Oliker, J. Shalf, and K. Yelick, “Optimization and performance modeling of stencil computations on modern microprocessors,” *SIAM Review*, vol. 51, no. 1, pp. 129–159, 2009.
- [15] D. Orozco, E. Garcia, and G. Gao, “Locality optimization of stencil applications using data dependency graphs,” in *Languages and Compilers for Parallel Computing*. Springer Berlin Heidelberg, 2011, pp. 77–91.
- [16] X. Zhou, “Tiling optimizations for stencil computations,” Ph.D. dissertation, University of Illinois at Urbana-Champaign, 2013. [Online]. Available: [http://polaris.cs.uiuc.edu/~zhou53/papers/Xing\\_Zhou.pdf](http://polaris.cs.uiuc.edu/~zhou53/papers/Xing_Zhou.pdf)
- [17] V. Bandishti, I. Pananilath, and U. Bondhugula, “Tiling stencil computations to maximize parallelism,” in *High Performance Computing, Networking, Storage and Analysis (SC), 2012 International Conference for*, Nov 2012, pp. 1–11.
- [18] L. Lamport, “The parallel execution of DO loops,” *Communications of the ACM*, vol. 17, no. 2, pp. 83–93, Feb. 1974. [Online]. Available: <http://doi.acm.org/10.1145/360827.360844>
- [19] D. G. Wonnacott, “Using time skewing to eliminate idle time due to memory bandwidth and network limitations,” in *International Parallel and Distributed Processing Symposium*, 2000, pp. 171–180.
- [20] A. Nguyen, N. Satish, J. Chhugani, C. Kim, and P. Dubey, “3.5-D blocking optimization for stencil computations on modern CPUs and GPUs,” in *Proceedings of the International Conference for High Performance Computing, Networking, Storage and Analysis*, 2010, pp. 1–13.
- [21] P. Balaprakash, A. Tiwari, and S. M. Wild, “Multi-objective optimization of HPC kernels for performance, power, and energy,” in *4th International Workshop on Performance Modeling, Benchmarking, and Simulation of HPC Systems*, 11/2013 2013.
- [22] P. Gschwandtner, J. Durillo, and T. Fahringer, “Multi-objective auto-tuning with Insieme: Optimization and trade-off analysis for time, energy and resource usage,” in *Euro-Par 2014 Parallel Processing*, ser. Lecture Notes in Computer Science. Springer International Publishing, 2014, vol. 8632, pp. 87–98. [Online]. Available: [http://dx.doi.org/10.1007/978-3-319-09873-9\\_8](http://dx.doi.org/10.1007/978-3-319-09873-9_8)